Research article

NMR IN BIOMEDICINE

Received: 1 May 2014, Revised: 25 January 2015, Accepted: 26 January 2015, Published online in Wiley Online Library

(wileyonlinelibrary.com) DOI: 10.1002/nbm.3278

Detection of lactate in the striatum without contamination of macromolecules by *J*-difference editing MRS at 7T

J. P. Wijnen[a]*, J. Haarsma[a,b], V. O. Boer[a], P. R. Luijten[a], S. van der Stigchel[c], S. F. W. Neggers[b] and D. W. J. Klomp[a]

Lactate levels are measurable by MRS and are related to neural activity. Therefore, it is of interest to accurately measure lactate levels in the basal ganglia networks. If sufficiently stable, lactate measurements may be used to investigate alterations in dopaminergic signalling in the striatum, facilitating the detection and diagnosis of metabolic deficits. The aim of this study is to provide a J-difference editing MRS technique for the selective editing of lactate only, thus allowing the detection of lactate without contamination of overlapping macromolecules. As a validation procedure, macromolecule nulling was combined with J-difference editing, and this was compared with J-difference editing with a new highly selective editing pulse. The use of a high-field (7T) MR scanner enables the application of editing pulses with very narrow bandwidth, which are selective for lactate. We show that, despite the sensitivity to B_0 offsets, the use of a highly selective editing pulse is more efficient for the detection of lactate than the combination of a broad-band editing pulse with macromolecule nulling. Although the signal-to-noise ratio of uncontaminated lactate detection in healthy subjects is relatively low, this article describes the test–retest performance of lactate detection in the striatum when using highly selective J-difference editing MRS at 7 T. The coefficient of variation, σ_w and intraclass correlation coefficients for within- and between-subject differences of lactate were determined. Lactate levels in the left and right striatum were determined twice in 10 healthy volunteers. Despite the fact that the test–retest performance of lactate detection is moderate with a coefficient of variation of about 20% for lactate, these values can be used for the design of new studies comparing, for example, patient populations with healthy controls. Copyright © 2015 John Wiley & Sons, Ltd.

Keywords: lactate; macromolecules; *J*-difference editing; MRS; 7 T

INTRODUCTION

The basal ganglia networks play an important role in the executive control over certain human behaviour, such as decision-making, response inhibition and selection (1,2). Failure in signal processing in these networks leads to neurological and psychiatric disorders, such as Parkinson's disease, Huntington's disease and obsessive–compulsive disorders, and can also explain various symptoms in psychotic disorders (3). These disorders are often linked to changes in the metabolic pathways of synaptic transmission (4,5). Therefore, the measurement of the activity of such pathways could aid in the scientific understanding and diagnosis of these diseases. MRS is capable of detecting neurotransmitters, such as glutamate and γ-aminobutyric acid (GABA), in the brain. The effect of these neurotransmitters is modulated by dopamine in the basal ganglia, which is, however, not detectable by MRS. In the early 1990s, lactate levels were found to be related to dopaminergic activity by microdialysis (6). Despite the fact that these findings did not prove a direct relationship between dopamine and lactate levels as measured by MRS, lactate levels remained of interest in studies of neural stimulation. For example, both Prichard *et al*. (7) and Sappey-Marinier *et al*. (8) detected an increase in lactate levels in the visual cortex after visual stimulation. These findings demonstrated the principle that lactate levels measured by MRS were related to neural activity. Therefore, it is important to accurately measure lactate levels in the basal ganglia. If sufficiently stable, lactate measurements might be used to detect alterations in dopaminergic signalling in the striatum, aiding the detection and diagnosis of metabolic deficits.

* *Correspondence to: J. P. Wijnen, Department of Radiology, University Medical Centre Utrecht, Heidelberglaan 100, 3508 GA Utrecht, the Netherlands. E-mail: jwijnen@umcutrecht.nl*

a *J. P. Wijnen, J. Haarsma, V. O. Boer, P. R. Luijten, D. W. J. Klomp*
Department of Radiology, University Medical Centre Utrecht, Utrecht, the Netherlands

b *J. Haarsma, S. F. W. Neggers*
Department of Psychiatry, University Medical Centre Utrecht, Utrecht, the Netherlands

c *S. van der Stigchel*
Department of Experimental Psychology, Utrecht University, Utrecht, the Netherlands

Abbreviations used: *3D, three-dimensional; ANOVA, random model analysis of variance; B_0, static magnetic field; B_1, applied magnetic field; CoV, coefficient of variation; CRLB, Cramer–Rao lower bound; FOCI, frequency offset-corrected inversion; FWHM, frequency width at half-maximum; GABA, γ-aminobutyric acid; ICC, intraclass correlation coefficient; LC, linear combination; MANOVA, multivariate analysis of variance; MM, macromolecule; MNI, Montreal Neurological Institute; NAA, N-acetylaspartate; ppm, parts per million; RF, radiofrequency; ROI, region of interest; semi-LASER, semi-localization by adiabatic selective refocusing; SNR, signal-to-noise ratio; TI, inversion time; VAPOR, variable pulse power and optimized relaxation delay.*

NMR IN BIOMEDICINE

Short-TE MRS, in combination with linear combination (LC)-model analysis, can be used to determine lactate levels in the brain with high sensitivity. This is not the most accurate method to assess lactate, however, as LC-model methods rely on the modelling of individual metabolite and macromolecular resonance signals. Furthermore, LC-model methods are prone to fitting errors, as a number of macromolecules (MMs) and lipids produce resonances that overlap with the low-intensity resonance of lactate (9–11). Moreover, contributions from MMs may be subject dependent. Although little is known about the role and appearance of MMs in different patient populations, the presence of such peaks could potentially have a significant effect on results obtained using LC-model analysis.

MRS editing techniques, such as J-difference editing, are used to eliminate signals from lipids that overlap with lactate signals. However, J-difference editing may still suffer from macromolecular contamination as some MMs are co-edited. This results in an overestimation of the lactate signal. MMs with resonances at 4.23 and 4.30 parts per million (ppm) are J-coupled to their resonances at 1.24 and 1.39 ppm, with J-coupling constants almost identical to that of lactate (11,12). In addition, threonine could be co-edited as its 4.2-ppm resonance is J-coupled to its 1.3-ppm resonance with a J-coupling constant of 6.3 Hz. As lactate at 4.10 ppm is coupled to 1.33 ppm, the co-editing of these MMs is hard to avoid (13). MM nulling can be used to remove macromolecular contributions at the expense of a subsequent loss in signal-to-noise ratio (SNR) as a result of relaxation of the longitudinal magnetization during the inversion recovery delay.

This article investigates whether the use of a high magnetic field strength (7 T) can improve J-difference editing. Higher spectral resolution at 7 T enables the use of highly selective refocusing pulses, whilst retaining high SNR. Typically, the low B_1^+ field available at high magnetic field strength results in narrow-bandwidth refocusing pulses that cause large chemical shift displacement errors, resulting in smaller volumes of effective editing. It has been shown previously, however, that J-difference editing can be highly efficient when using frequency offset-corrected inversion [FOCI (14)] (13).

The aim of this study was to provide an improved J-difference editing technique for lactate by excluding signals of co-edited MMs. The gain in SNR of a semi-localization by adiabatic selective refocusing (semi-LASER) editing sequence with refocusing FOCI pulses can be used to measure lactate in the striatum of the human brain at 7 T, whilst excluding the influence of co-edited MMs. Furthermore, the sensitivity of this method for the determination of lactate levels in the striatum was assessed by a test–retest study. The results of the test–retest study provide an input for power calculations in future studies involving accurate lactate measurements.

METHODS

Hardware and subjects

All investigations were performed on a 7T whole-body MR system (Philips, Cleveland, OH, USA). A birdcage transmit head coil (Nova Medical, Inc., Burlington, MA, USA) with two independent transmit channels was used in combination with a 32-channel receive coil (Nova Medical, Inc.). With this coil set-up, it was possible to achieve a B_1^+ value of 20 μT in the striatum of the human brain.

Lactate levels in the brain were investigated in 10 healthy volunteers (aged 35 ± 12 years). Measurements were performed twice to determine the test–retest performance of the lactate editing sequence. The time interval between the repeated measurements varied between 1 week and 6 months. The participants in this study were a subset of a larger cohort in which MRI examinations were also performed at 3 T. Therefore, a high-resolution three-dimensional (3D) T_1-weighted image of all participants was available for segmentation. All participants gave informed consent prior to the MRI examinations.

MRI and MRS protocol

To generate the required B_1^+ field of 20 μT in the area of interest (basal ganglia), the transmit phase difference between channels was optimized as described previously (15). After radiofrequency (RF) shimming, a 3D T_1-weighted background image was made over which the MRS volume ($40 \times 25 \times 24\ mm^3$) was positioned. B_0 shimming of the voxel with second-order shim fields was performed automatically by the Philips pencil beam volume algorithm, similar to FASTERMAP shimming (16,17).

A semi-LASER sequence was used for lactate editing. FOCI pulses (foci factor 10) were used for refocusing of the signal. FOCI pulses were generated based on a hyperbolic secant pulse using a B_{1max} value of 20 μT as described previously (13). The large bandwidth of the FOCI pulses (16.8 kHz) enabled efficient editing as a result of minimal chemical shift displacement errors (4.7%) of the CH (4.10 ppm) and CH_3 (1.33 ppm) resonances of lactate. TE = 144 ms and TR = 5200 ms (shortest TR possible within specific absorption rate limits). The resulting acquisition time, including 150 signal averages, was 13 min.

Two approaches to eliminate the co-editing of MMs were compared. In the first, MM contributions were suppressed by nulling their signal using an RF inversion pulse before J-difference editing. In the second, a highly selective editing pulse, which refocuses the 4.1-ppm resonance of lactate without perturbing the 4.23- and 4.30-ppm coupling partners of MM2 and MM3, was used to avoid co-editing of MMs.

MM nulling

A broad-band refocusing pulse was created for simultaneous water suppression and J-difference editing. The editing pulse had one broad refocusing band [frequency width at half-maximum (FWHM), 1000 Hz] centred at 4.7 ppm for water suppression and refocusing of the 4.10-ppm resonance of lactate. To investigate the contribution of MM2 and MM3 to the edited signal, an inversion recovery experiment was performed. The inversion recovery was combined with J-difference editing (TE = 144 ms) using the broad-band refocusing pulse. A non-localized adiabatic inversion pulse with a duration of 7.8 ms was applied. This adiabatic full-passage pulse consisted of a linear ramp with an amplitude of 1.2 ms, followed by a plateau for 5.4 ms and a linear downward ramp lasting for 1.2 ms; the frequency sweep was 1878 Hz and B_{1max} was 20 μT. According to literature values, the T_1 value of MMs in the human brain is approximately 400 ms at 7 T (18). To assess T_1 more precisely for the co-edited MMs in the striatum in the human brain, three points at the inversion recovery curve close to the expected point of nulling were sampled using T_1 values of 270, 358 and 435 ms. The relative phase between the lactate and MM signals at 1.2–1.4 ppm was used to tune the optimal inversion time (TI) for nulling of the MM signals: TI was too short if the relative phase was 0° and too long if the relative phase was 180°.

Highly selective editing

A new editing pulse was designed to enable editing of lactate only. Therefore, a single-band Shinnar Le-Roux pulse was designed for J-difference editing of lactate. This pulse had a duration of 38 ms and FWHM of the inversion frequency profile was 30 Hz (Fig. 1B). In the 'edit on' condition, the editing pulse was centred at the 4.10-ppm resonance of lactate; in this way, co-editing of MM2 at 4.23 ppm was avoided. In the 'edit off' condition, the editing pulse was applied 1000 Hz off-resonance (at 8.0 ppm). The narrow-band editing sequence was preceded by a variable pulse power and optimized relaxation delay (VAPOR) sequence for water suppression.

Regions of interest (ROIs) and segmentation

Voxels of 24 cm^3 ($24 \times 25 \times 40$ mm^3) were positioned in the basal ganglia of the right and left hemisphere, covering most of the striatum (caudate nucleus and putamen), smaller parts of the globus pallidus and the substantia nigra pars compacta, without including cerebrospinal fluid in the voxels (Fig. 2).

To calculate the grey matter volume of the globus pallidus, caudate nucleus and putamen in the voxels, we used 3D T_1-weighted images acquired from the same subjects at 3 T. These images were normalized in MNI (Montreal Neurological Institute) space using MRIcron. A manual segmentation was performed on the averaged (over subjects) 3-T 3D T_1-weighted images (Fig. 2). The 3-T 3D T_1-weighted MR images were used for this process, as the image quality for segmentation in the basal ganglia was better for the 3-T images because of the more homogeneous B_1 RF field compared with the 7-T images. The population average T_1 was used because individual subcortical areas were too noisy for fully automated segmentation. Normalization and averaging over the population led to averaging out of noise and resulted in an image that could be more accurately segmented based on the contrast between grey and white matter.

SPM8 was used for image normalization and registration (Functional Imaging Laboratory, University College London, London, UK). The manually segmented mean ROIs (globus pallidus, caudate nucleus and putamen) were inverse normalized to the individual participant's brain [using 'unified

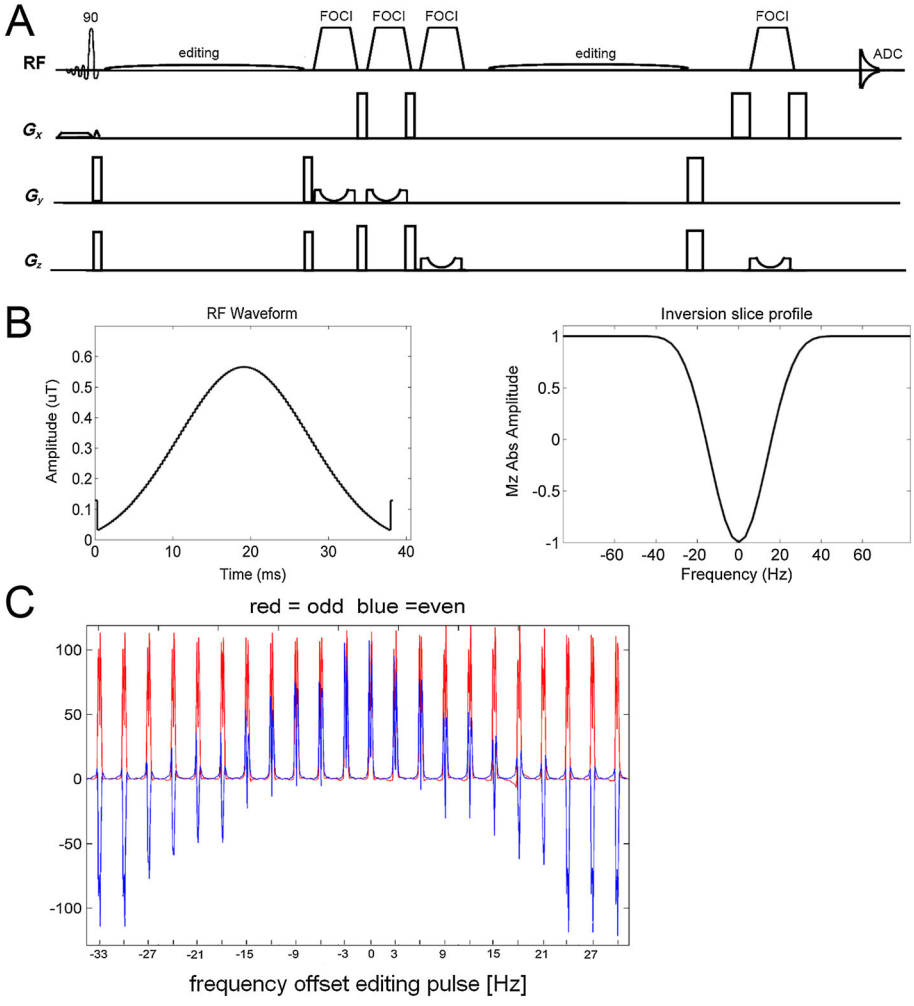

Figure 1. (A) Pulse sequence of semi-localization by adiabatic selective refocusing (semi-LASER) J-difference editing sequence with frequency offset-corrected inversion (FOCI) refocusing pulses and crusher gradients. This sequence is preceded by a variable pulse power and optimized relaxation delay (VAPOR) water suppression sequence. (B) Radiofrequency (RF) waveform and slice inversion profile of the editing pulse. The pulse has a duration of 38 ms and the frequency width at half-maximum (FWHM) of the inversion profile is 30 Hz. (C) Series of phantom experiments to determine the editing efficiency and B_0 offset effects of the narrow-bandwidth editing pulse shown in (B). Red are odd spectra, and blue are even spectra. These have opposite phase, but are displayed in the same phase for comparison. The subtraction of the two generates the edited spectrum. The offset of the editing pulse was varied in steps of 3 Hz between each pair of blue and red spectra.

NMR IN BIOMEDICINE

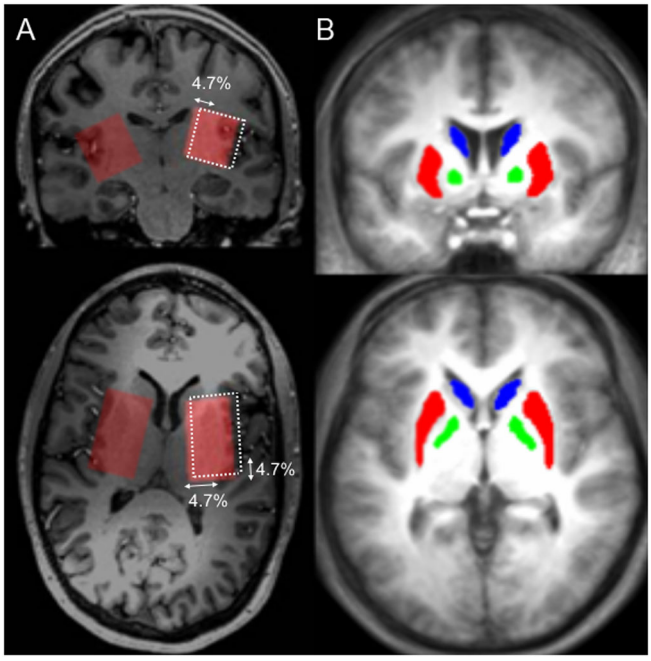

Figure 2. (A) Position of the MRS voxel in the striatum of the right and left hemisphere. The chemical shift displacement error between the two coupled spin systems of lactate of 4.7% in the two refocusing directions is schematically drawn (not to scale). As a result of this chemical shift displacement error, the volume on which the editing is effective is reduced by approximately 9%. (B) The different basal ganglia nuclei were segmented on an averaged T_1 scan. Putamen is in red, caudate is in blue and globus pallidus is in green.

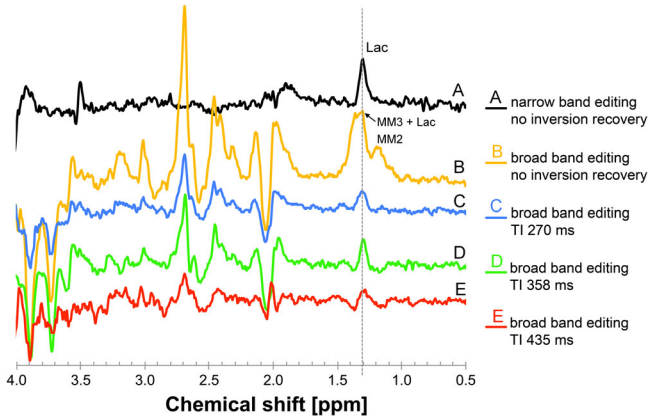

Figure 3. Inversion recovery series of the edited spectrum in the striatum. The top two MR spectra (A, B) were acquired without inversion recovery with the narrow-band and broad-band editing pulses, respectively. The bottom three MR spectra (C–E) were acquired with a broad-band inversion at inversion times (TI) of 270, 358 and 435 ms, respectively. All MR spectra were obtained from a $24 \times 25 \times 40\text{-mm}^3$ voxel in the striatum with 128 averages; spectra are normalized to noise. The MR spectra shown in (A) and (D) are from the same volunteer, those in (B) and (C) from another volunteer and that in (E) from yet another volunteer. It should be noted that the peaks labelled MM2 and MM3 probably also contain alanine and threonine residues in proteins, as these large molecules cause signal with a broad linewidth.

segmentation'-derived inverse normalization parameters (19)], and then co-registered to the 7T T_1-weighted individual images. This segmentation could then be used to calculate the amount of grey matter, white matter and cerebrospinal fluid in the MRS voxels for every individual (in-house-developed Matlab program). These amounts were used to correct the metabolite levels for differences in the relaxation of water in grey and white matter, as well as different partial volumes of grey and white matter.

MRS data analysis

The signals of the 32 receiver coils were combined after amplitude weighting and phasing based on the water reference signal. The water reference signal was also used for eddy current correction and as an internal standard for quantification. Each acquisition was frequency aligned with the singlet resonance of N-acetylaspartate (NAA). The acquisitions were averaged after correction. The sum of all averaged odd and even scans resulted in an MR spectrum displaying all metabolites, except lactate (metabolite spectrum). The subtraction of all averaged odd and even scans resulted in an MR spectrum displaying the lactate signal (edited spectrum) (Fig. 3). Residual water filtering, phasing and fitting of the metabolite and edited spectra were implemented using Matlab. The NAA peak in the metabolite spectrum was fitted with a Lorentzian singlet, and the frequency, linewidth and phase of the NAA singlet were used as prior knowledge to fit the lactate peak in the edited spectrum. Lactate was fitted with a Lorentzian doublet (^{1}H–^{1}H scalar coupling constant, 7 Hz). Creatine and choline were also fitted with Lorentzian lines. Cramer–Rao lower bounds (CRLBs) of the fits were calculated as a lower boundary of fitting accuracy (20).

In addition to correction for different water content and relaxation in grey matter and white matter, the metabolite levels were also corrected for metabolite T_1 and T_2 relaxation. The T_2 value of water in the voxel of interest was determined with a semi-LASER TE series (TE = 33–313 ms, steps of 20 ms), and literature values were used for the T_1 values of water and the T_1 and T_2 values of metabolites (21–24). The T_1 values of NAA, creatine and choline in grey matter/white matter were 1900/1800, 1780/1800, and 1500/1320, respectively. The T_2 values of NAA, creatine and choline in grey matter/white matter were 130/158, 90/109 and 121/109 ms, respectively. The T_1 value of lactate was assumed to be similar to the T_1 value of choline. The T_2 value of lactate was assumed to be similar to the T_2 value of singlets in the basal ganglia, as reported by Marjanska *et al.* (24) Therefore, we used a T_1 value of 1500 ms and T_2 value of 100 ms for lactate.

Statistical analysis

Means and standard deviations, as well as the coefficient of variation (CoV), of the metabolite levels (corrected for grey and white matter fraction) were determined. The CoV was defined as the standard deviation of differences between the first and second measurement (D_k) divided by the mean value of all measurements (M) in each voxel, for each metabolite level (25), or:

$$\mathrm{CoV} = \frac{\sqrt{\frac{1}{(n-1)}\sum_{k=1}^{n}\left(D_k - \overline{D}\right)^2}}{\overline{M}} \cdot 100 \text{ and } \overline{D} = \frac{1}{n}\sum_{k=1}^{n} D_k \qquad [1]$$

where k delineates the specific volunteer and n refers to the total number of volunteers.

A repeated-measures multivariate analysis of variance (MANOVA) was used to examine systematic changes in metabolite levels across measurements. The within-subject variation in metabolite levels was analysed using the within-subject standard deviation. The within-subject standard deviation and its standard error can be estimated by:

$$\sigma_w = \sqrt{\frac{\sum_{i=1}^{n}\sigma_i^2}{n}} \quad [2]$$

with

$$\mathrm{SE}_{\sigma_w} = \frac{\sigma_w}{\sqrt{2n(m-1)}} \quad [3]$$

where σ_i^2 is the variance in the value of interest on repeated testing for subject i, n denotes the total number of subjects in the sample and m represents the total number of repeated measurements. The within-subject standard deviation represents the average variability of an individual's values on repeated testing. It is expressed in the same units as the measured value, which is mM in this study (26).

To assess the reproducibility for each metabolite, a reliability analysis was performed (SPSS 20.0.0). The reliability analysis used a two-way random model analysis of variance (ANOVA), with the subjects and repeated measurements as factors of variance. The analysis also included a random noise term. Using this method, the within-subject variance $\sigma^2_{\mathrm{within}}$ (repeated measurements), between-subject variance $\sigma^2_{\mathrm{between}}$ (subject to subject) and intraclass correlation coefficient (ICC) were calculated. The overall measurement variance can be expressed as:

$$\sigma^2 = \sigma^2_{\mathrm{between}} + \sigma^2_{\mathrm{within}} + \sigma^2_{\mathrm{random}}, \quad [4]$$

where $\sigma^2_{\mathrm{random}}$ reflects the variance caused by randomness. We defined $\mathrm{ICC}_{\mathrm{between}}$ to reflect the part of the total variance that is caused by subject to subject effects, and $\mathrm{ICC}_{\mathrm{within}}$ to represent the part of the total variance that is caused by differences in the repeated measurement by the following equations:

$$\mathrm{ICC}_{\mathrm{between}} = \mathrm{MS}_{\mathrm{between}}/(\mathrm{MS}_{\mathrm{between}} + \mathrm{MS}_{\mathrm{within}} + \mathrm{MS}_{\mathrm{random}}) \times 100\% \quad [5]$$

$$\mathrm{ICC}_{\mathrm{within}} = \mathrm{MS}_{\mathrm{within}}/(\mathrm{MS}_{\mathrm{between}} + \mathrm{MS}_{\mathrm{within}} + \mathrm{MS}_{\mathrm{random}}) \times 100\% \quad [6]$$

MS is the mean square, which represents the sum of squares (σ^2) divided by the number of degrees of freedom. For the sake of completeness, $\mathrm{ICC}_{\mathrm{random}}$ can be calculated from Equations [5] and [6], being 100% minus $\mathrm{ICC}_{\mathrm{between}}$ and $\mathrm{ICC}_{\mathrm{within}}$.

RESULTS

J-difference editing of lactate

Phantom measurements

The narrow-band editing pulse was tested on a phantom filled with water and a high concentration of lactate (~100 mM). Figure 1C shows the off-resonance performance of the pulse. Odd spectra (editing pulse centred at 4.1 ppm) are shown in red and even spectra (editing pulse centred at 8 ppm) are shown in blue. The frequency offset between each pair of MR spectra is 3 Hz. The editing efficiency (signal at 1.3 ppm of the odd spectrum subtracted from the even spectrum versus twice the even spectrum) was 85%. A B_0 offset of 3 Hz results in 75% editing efficiency; an offset of 9 Hz results in 60% editing efficiency. As a result of the chemical shift displacement error of 4.7% between the two coupled spin systems of lactate in two refocusing directions, the volume on which the editing is effective is reduced by ~9% [1 – $(0.953)^2$]. In two of the remaining compartments of the chemical shift displacement error, the signal of lactate will be reversed, causing another 8% further reduction in the edited lactate signal.

In vivo measurements

Figure 3A clearly shows the NMR resonance of lactate without any contamination from macromolecular signals at 1.3 ppm as obtained with the sequence using highly selective editing pulses. In the MR spectrum of the broad-band refocusing pulses, in addition to the resonances of lactate, the co-edited resonances of MMs at 1.24 ppm (MM2) and 1.39 ppm (MM3) are visible (Fig. 3B). Furthermore, the peak around 1.33 ppm in the broad-band refocused MR spectrum (Fig. 3B) seems to be shifted towards 1.4 ppm, which indicates that the broad resonance of MM3 most likely overlaps with the lactate resonance. When nulling the resonances of MMs with a single inversion at TI = 270 ms, MM2 and MM3 are still visible and have the same phase as the lactate signal (Fig. 3C). This means that a TI of 270 ms is too short to null the macromolecular peaks. In the MR spectra obtained with TI = 358 and 435 ms, the resonances of MMs have an opposite phase to the lactate peak; however, it is unclear how much of the lactate signal is still overlapped by MMs. Of all the inversion recovery-based scans with broad-band refocusing pulses (Fig. 3B–E), the MR spectrum in Figure 3D comes closest to full MM nulling. This indicates that the optimal TI is between 270 and 358 ms. An AMARES (27) fit of the signal at 1.3 ppm resulted in the following values (a.u.): 2.6, 10.7, 1.46, 1.42 and 0.7 for the MR spectra in Figure 3A–E, respectively.

The edited and non-edited MR spectra of the striatum obtained with the narrow-band editing pulse are shown in Figure 4. The signals from NAA, creatine and choline have high SNR despite the long TE and are not affected by the editing pulse.

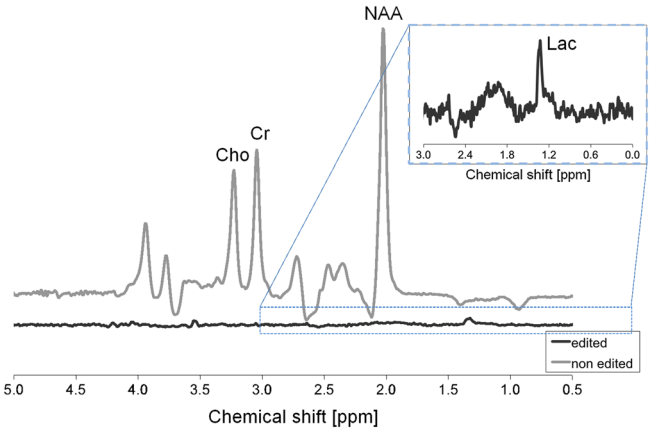

Figure 4. Example of added and subtracted spectra in one volunteer. The metabolite spectrum is shown in grey and the edited spectrum is shown in black and enlarged in the inset. A clear and sharp signal for lactate can be observed at 1.3 ppm. Cho, choline; Cr, creatine; Lac, lactate; NAA, N-acetylaspartate.

Table 1. Descriptive statistics of MRS measurements in the left and right hemispheres of 10 subjects

		Lactate		N-Acetylaspartate		Creatine		Choline	
Hemisphere	Parameter	Session 1	Session 2	Session 1	Session 2	Session 1	Session 2	Session 1	Session 2
Right	Mean (mM)	0.46	0.45	9.99	10.65	7.49	8.04	2.16	2.27
	SD (mM)	0.08	0.05	0.87	1.28	0.75	1.25	0.17	0.27
	CoV (%)	18	12	9	12	10	16	8	12
	σ_w (mM)	0.03		0.53		0.55		0.15	
	$SE_{\sigma w}$	0.01		0.12		0.12		0.03	
	σ_w (%)	6.36		5.13		7.07		6.76	
Left	Mean (mM)	0.47	0.46	11.32	11.63	8.99	9.05	2.60	2.64
	SD (mM)	0.11	0.06	1.77	2.06	1.20	1.31	0.30	0.45
	CoV (%)	24	13	16	18	13	15	11	17
	σ_w (mM)	0.06		0.77		0.63		0.21	
	$SE_{\sigma w}$	0.01		0.17		0.14		0.05	
	σ_w (%)	13.07		6.70		7.04		7.89	

CoV, coefficient of variation; SD, standard deviation; SE, standard error.

These metabolites were also quantified and the results are presented in Table 1.

Descriptive statistics

The grey matter fractions in the voxel of the right hemisphere in sessions 1 and 2 were 0.29 ± 0.02 and 0.32 ± 0.03, respectively (Student's t-test, $p = 0.02$). The grey matter fractions in the voxel of the left hemisphere in sessions 1 and 2 were 0.32 ± 0.04 and 0.30 ± 0.09, respectively (Student's t-test, $p = 0.63$).

Reproducibility was assessed using the editing sequence based on selective refocusing of exclusively the coupled spins at 4.1 ppm. The averages and standard deviations of the metabolite levels for the first and second sessions in the voxels of the left and right hemispheres are listed in Table 1. The average CRLBs of the fit of the metabolites were 2.3, 1.8, 2.1 and 3.7 for NAA, creatine, choline and lactate, respectively.

CoV, σ_w and its standard error, $ICC_{between}$ and ICC_{within} are summarized in Tables 1 and 2. It should be noted that CoV and σ_w of lactate are in the same range as the corresponding values for the other metabolites. $ICC_{between}$ for lactate is a factor of 3 higher than ICC_{within}, whereas this is not the case for the other metabolites. The residual variation (ICC_{random}) can be assigned to measurement inaccuracies. ICC_{random} is largest for lactate, the signal with lowest SNR, and lowest for NAA, the signal with highest SNR.

A correlation plot between measurements 1 and 2 of lactate and NAA in the left and right hemisphere voxels is shown in Figure 5. A large $ICC_{between}$ is reflected in the large data spread along the broken diagonal line (Table 2). A large ICC_{within} is reflected in the large data spread perpendicular to the broken diagonal line (Table 2).

DISCUSSION

The detection of metabolites, such as lactate, in the normal brain is challenging. This is not only because of its low concentration (and therefore low SNR), but also because of the fact that the lactate MR signal overlaps with signals from other, more highly concentrated compounds. These include lipids and MMs. Several methods to measure lactate are available, such as short- and long-TE MRS (28), J-difference editing (29,30) and multiple quantum coherence editing (31–33). The direct detection methods need to be combined with LC-model analysis. This is not straightforward as the signal of lactate is small compared with the signals of overlapping MMs. As the lactate level is strongly influenced by the fitting of MMs, the accuracy in detecting the static pool of lactate with these direct detection techniques is questionable (32). In addition, when using a long TE, the SNR of lactate is further reduced because of T_2 relaxation (signal loss of ~68% when comparing TE = 30 ms and TE = 144 ms and assuming $T_2 = 100$ ms). This also complicates the LC-model analysis. As shown by Near *et al.* (34) in a comparison of J-difference editing and direct detection of GABA in the brain, the metabolite level of GABA obtained with direct detection shows substantial bias in the results. The results depend on SNR and linewidth,

Table 2. Results of the reliability analysis. The intraclass correlation coefficients (ICCs) are calculated from the two-way random model analysis of variance (ANOVA)

Hemisphere	Parameter	Lactate	N-Acetylaspartate	Creatine	Choline
Right + left	$ICC_{between}$	42	60	57	56
	ICC_{within}	14	27	25	25
	ICC_{random}	44	13	19	20

$ICC_{between}$ reflects the part of the total variance that is caused by subject to subject effects; ICC_{within} represents the part of the total variance that is caused by the differences in the repeated measurements (Equations [4]–[6]).

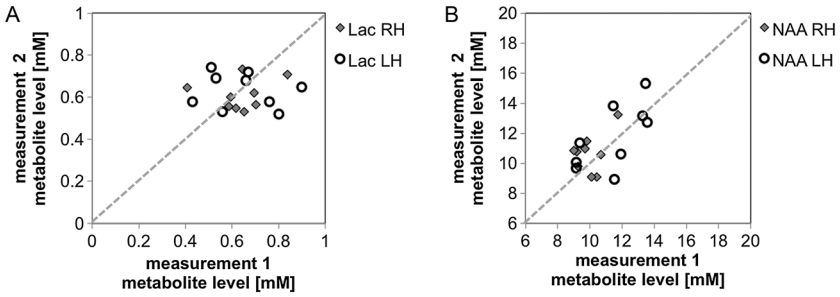

Figure 5. Correlation between metabolite levels in measurements 1 and 2 [in voxel in left (LH) and right (RH) hemisphere] for lactate (Lac) (A) and N-acetylaspartate (NAA) (B).

even with constant overlapping resonances. Using J-difference editing methods, it is possible to obtain the lactate signal without overlapping resonances, allowing the use of a simple fitting routine for quantification of the signal. However, as the lactate spectrum results from the subtraction of two spectra, this method is prone to subtraction artefacts. Differences between the two spectra caused by, for example, motion may lead to an incorrect assignment of the subtraction residue to lactate. Furthermore, relatively small B_0 offsets diminish efficient editing as shown in the phantom measurements of this study. In lipid-rich environments, such as tumour tissue and breast tissue, the T_2 value of lactate can be reduced (35), leading to a substantial loss of the lactate signal. Multiple quantum coherence methods allow for gradient dephasing of overlapping singlet signals, and hence can specifically detect lactate within a single shot (32). Unfortunately, by selecting the double-quantum coherence pathway as a means of editing, at least 50% of the initial signal is lost (36). Furthermore, without the use of highly selective refocusing pulses, MM2 and MM3 can still be co-edited.

In view of these considerations, we chose to unambiguously detect lactate exclusively using J-difference editing despite the loss of signal caused by the long TE and the sensitivity to B_0 offsets. As demonstrated, this can be performed by either combining MM nulling with J-difference editing to remove macromolecular co-editing, or by using a highly selective editing pulse that edits lactate only.

This study shows that, when using J-difference editing, MM co-editing is substantial when the bandwidth of the editing pulse is not sufficiently narrow. Moreover, when trying to null the co-edited macromolecular signal with an inversion pulse, the apparent T_1 value of MMs is longer than anticipated based on literature data (18,30). This could be related to the fact that MM2 and MM3 resonances may be partially attributable to alanine and threonine residues in proteins. Complete nulling of MMs remains questionable, even when fine-tuning the nulling by choosing different TI values. A small variation in TI leads to a large variation in the 'lactate' signal amplitude at 1.3 ppm, as shown by the fitted results of the MR spectra in Figure 3. Therefore, MM nulling may not be the preferred method to obtain an accurate measure for lactate. The nulling procedure can be inaccurate as the true MM T_1 value is unknown. Also, depending on the TI, 40–60% of the metabolite signal is lost as a result of longitudinal relaxation.

The high spectral dispersion at 7 T facilitates the use of narrow-band RF editing pulses that can select lactate signals without contamination of other overlapping signals. The highly selective RF pulses are very sensitive to B_0 offsets (for example, caused by motion) and therefore require a stable field. Nevertheless, the efficiency when using such a narrow-band RF pulse remains higher than with the inversion recovery sequence, even up to a B_0 offset of 9 Hz. Selective J-difference editing measurements might be improved even further by enabling accurate B_0 drift correction techniques. It should be noted that substantial field offsets lead to efficiency loss and additional co-editing of threonine. The threonine resonance at 1.3 ppm is coupled to 4.2 ppm with a J-coupling constant of 6.3 Hz. Therefore, threonine could be (partially) co-edited if a B_0 offset of 30 Hz occurs. In that case, it is not possible to distinguish threonine from lactate, or threonine is mistakenly identified as lactate.

The sensitivity of the J-difference editing technique with highly selective editing pulses to measure striatal lactate levels in a group of healthy volunteers was assessed after demonstrating that lactate could be unambiguously detected. A rather large voxel and long acquisition time were used to acquire the lactate signal under baseline conditions. Other studies have reported changes in lactate levels in activated brain tissue using smaller voxels and shorter acquisition times (37–39). According to the work of Lin *et al.* (39), the lactate signal changes by 15% on visual stimulation. Considering the repeatability results of this study, the selective J-difference editing technique, with σ_w of 13% and CoV of 12–23%, is a promising method for the detection of such a difference on an individual basis. In contrast with functional MRS studies (37–39), highly selective J-difference editing can detect absolute levels of lactate, facilitating subject or group comparisons. Moreover, studies that use short-TE MRS rely on the modelling of lactate and MMs in LC-model analysis. However, the exact resonance position of MMs is sometimes unclear as, for example, different frequencies have been reported for MM3 (11,12). In dynamic MRS studies that used short TEs, it was assumed that the contribution of the MMs did not change over time and was not affected by the applied physiological stimuli (40). Furthermore, it is known that the blood oxygen level-dependent effect influences the spectral linewidth in activated brain tissue (38,41). To compensate for this effect, all MR spectra (rest and activation) can be line broadened before subtraction (38,39). However, the effect of line broadening on the coupled spin system of the different MMs will be difficult to assess. It is uncertain whether the line broadening caused by the blood oxygen level-dependent effect is equal for metabolites and MMs. This adds additional complexity to the above-mentioned LC-model analysis.

The reproducibility of edited lactate in the normal brain has not been reported previously. In a study by McLean *et al.* (42), the repeatability of edited lactate in astrocytomas was examined at 3 T. The CoV was 16% for lactate versus 10% for NAA. Considering that the lactate levels in astrocytomas are about 10-fold higher than in the normal brain, it can be expected that the

CoV of edited lactate in the normal brain will be higher, even when measured at a stronger magnetic field. In our study, the CoV of lactate was between 12% and 23%, varying between sessions and between left and right hemispheres. This is somewhat larger than the CoV of the metabolites (NAA, choline, creatine), which ranged between 8% and 18%, depending on session and hemisphere (Table 1); this can be expected as NAA, choline and creatine have higher SNRs. One study has reported a CoV of approximately 13% for GABA, which has a higher SNR than lactate, measured with J-difference editing in the prefrontal cortex and anterior cingulate at 7 T (43).

The σ_w value of lactate, a measure of within-subject variation, was 6% of the mean lactate value in the right hemisphere, and 12% of the mean value in the left hemisphere. For the metabolites NAA, creatine and choline, there was no such large difference in σ_w between the left and right hemisphere voxels. This observation for lactate may be a random effect; the SNR is relatively low, and we do not expect different lactate levels in the left and right hemispheres.

The repeatability of NAA, creatine and choline was assessed by the editing sequence. The CoV of these metabolites was comparable with that of lactate, which might seem unexpected when considering the much higher SNR of these signals in the MR spectrum. Also, in a previous study, short-TE semi-LASER at 7 T proved to be highly reproducible across multiple vendors and centres (44). However, the editing sequence had a TE of 144 ms, which was only optimal for the J-coupling pattern of lactate. Also, single Lorentzian lines were fitted to the resonance positions of 2.0, 3.0 and 3.2 ppm, whereas, at these frequencies, multiple additional resonances and macromolecular peaks are present that were not taken into account. The difference in grey matter fraction in the right hemisphere voxel between the first and second measurements could also be a cause of the rather large CoV of NAA, creatine and choline.

The ANOVA revealed that ICC_{within} is smaller than $ICC_{between}$. However, for lactate, it is questionable whether we were able to detect the differences within this group of healthy volunteers as ICC_{random}, which reflects the noise level of the measurement, was equal to $ICC_{between}$. The other metabolites were detected with higher SNR, as reflected in a lower ICC_{random}. Therefore, even with this suboptimal method to detect NAA, creatine and choline, differences between and within subjects can be distinguished.

CONCLUSIONS

We have presented a J-difference editing MRS method for the detection of lactate in the brain without contamination of MMs. We assessed measures for the test–retest performance of this method to determine lactate levels in the striatum of the brain in a healthy population. Although the variability in a healthy population is rather high, these values can still be used to design new studies comparing patient populations, in which lactate levels of the striatum are expected to deviate more than in a healthy population, with healthy controls.

Acknowledgements

We gratefully acknowledge funding from an intramural grant from the Neuroscience and Cognition Utrecht programme awarded to S. F. W. Neggers, S. van der Stigchel and D. W. J. Klomp.

REFERENCES

1. Dodd NJ, Moore JV, Poppitt DG, Wood B. In vivo magnetic resonance imaging of the effects of photodynamic therapy. Br. J. Cancer 1989; 60(2): 164–167.
2. Lagemaat MW, Maas MC, Vos EK, Bitz AK, Orzada S, Weiland E, van Uden MJ, Kobus T, Heerschap A, Scheenen TW. 31P MR spectroscopic imaging of the human prostate at 7 T: T relaxation times, nuclear Overhauser effect, and spectral characterization. Magn. Reson. Med. 2014. doi: 10.1002/mrm.25209.
3. Shepherd GM. Grey matter. Corticostriatal connectivity and its role in disease. Nat. Rev. Neurosci. 2013; 14(4): 278–291.
4. Toru M, Nishikawa T, Mataga N, Takashima M. Dopamine metabolism increases in post-mortem schizophrenic basal ganglia. J. Neural Transm. 1982; 54(3–4): 181–191.
5. Benes FM. Emerging principles of altered neural circuitry in schizophrenia. Brain Res. Brain Res. Rev. 2000; 31(2–3): 251–269.
6. Takita M, Mikuni M, Takahashi K. Habituation of lactate release responding to stressful stimuli in rat prefrontal cortex in vivo. Am. J. Physiol. 1992; 263(3 Pt 2): R722–727.
7. Prichard J, Rothman D, Novotny E, Petroff O, Kuwabara T, Avison M, Howseman A, Hanstock C, Shulman R. Lactate rise detected by ^{1}H NMR in human visual cortex during physiologic stimulation. Proc. Natl. Acad. Sci. U. S. A. 1991; 88(13): 5829–5831.
8. Sappey-Marinier D, Calabrese G, Fein G, Hugg JW, Biggins C, Weiner MW. Effect of photic stimulation on human visual cortex lactate and phosphates using ^{1}H and ^{31}P magnetic resonance spectroscopy. J. Cerebral Blood Flow Metab. 1992; 12(4): 584–592.
9. Tkac I, Oz G, Adriany G, Ugurbil K, Gruetter R. In vivo ^{1}H NMR spectroscopy of the human brain at high magnetic fields: metabolite quantification at 4 T vs. 7 T. Magn. Reson. Med. 2009; 62(4): 868–879.
10. Osbakken MD, Kreider JW, Taczanowsky P. Nuclear magnetic resonance imaging characterization of a rat mammary tumor. Magn. Reson. Med. 1986; 3(1): 1–9.
11. Pfeuffer J, Tkac I, Provencher SW, Gruetter R. Toward an in vivo neurochemical profile: quantification of 18 metabolites in short-echo-time (1)H NMR spectra of the rat brain. J. Magn. Reson. 1999; 141(1): 104–120.
12. Behar KL, Rothman DL, Spencer DD, Petroff OA. Analysis of macromolecule resonances in ^{1}H NMR spectra of human brain. Magn. Reson. Med. 1994; 32(3): 294–302.
13. Arteaga de Castro CS, Boer VO, Andreychenko A, Wijnen JP, van der Heide UA, Luijten PR, Klomp DW. Improved efficiency on editing MRS of lactate and gamma-aminobutyric acid by inclusion of frequency offset corrected inversion pulses at high fields. NMR Biomed. 2013; 26(10): 1213–1219.
14. Ordidge RJ, Wylezinska M, Hugg JW, Butterworth E, Franconi F. Frequency offset corrected inversion (FOCI) pulses for use in localized spectroscopy. Magn. Reson. Med. 1996; 36(4): 562–566.
15. Boer VO, van Lier AL, Hoogduin JM, Wijnen JP, Luijten PR, Klomp DW. 7-T (1) H MRS with adiabatic refocusing at short TE using radiofrequency focusing with a dual-channel volume transmit coil. NMR Biomed. 2011; 24(9): 1038–1046.
16. Gruetter R Automatic, localized in vivo adjustment of all first- and second-order shim coils. Magn. Reson. Med. 1993; 29(6): 804–811.
17. Shen J, Rycyna RE, Rothman DL. Improvements on an in vivo automatic shimming method [FASTERMAP]. Magn. Reson. Med. 1997; 38(5): 834–839.
18. Xin L, Schaller B, Mlynarik V, Lu H, Gruetter R. Proton T1 relaxation times of metabolites in human occipital white and gray matter at 7 T. Magn. Reson. Med. 2013; 69(4): 931–936.
19. Ashburner J, Friston KJ. Unified segmentation. Neuroimage 2005; 26(3): 839–851.
20. Cavassila S, Deval S, Huegen C, van Ormondt D, Graveron-Demilly D. Cramer–Rao bounds: an evaluation tool for quantitation. NMR Biomed. 2001; 14(4): 278–283.
21. Rooney WD, Johnson G, Li X, Cohen ER, Kim SG, Ugurbil K, Springer CS Jr. Magnetic field and tissue dependencies of human brain longitudinal $^{1}H_2O$ relaxation in vivo. Magn. Reson. Med. 2007; 57(2): 308–318.
22. Bartha R, Michaeli S, Merkle H, Adriany G, Andersen P, Chen W, Ugurbil K, Garwood M. In vivo $^{1}H_2O$ T2+ measurement in the human occipital lobe at 4 T and 7 T by Carr–Purcell MRI: detection of microscopic susceptibility contrast. Magn. Reson. Med. 2002; 47(4): 742–750.

23. Otazo R, Mueller B, Ugurbil K, Wald L, Posse S. Signal-to-noise ratio and spectral linewidth improvements between 1.5 and 7 Tesla in proton echo-planar spectroscopic imaging. Magn. Reson. Med. 2006; 56(6): 1200–1210.
24. Marjanska M, Auerbach EJ, Valabregue R, Van de Moortele PF, Adriany G, Garwood M. Localized ^{1}H NMR spectroscopy in different regions of human brain in vivo at 7 T: T2 relaxation times and concentrations of cerebral metabolites. NMR Biomed. 2012; 25(2): 332–339.
25. Bland JM, Altman DG. Statistical methods for assessing agreement between two methods of clinical measurement. Lancet 1986; 327 (8476): 307–310.
26. Zandbelt BB, Gladwin TE, Raemaekers M, van Buuren M, Neggers SF, Kahn RS, Ramsey NF, Vink M. Within-subject variation in BOLD-fMRI signal changes across repeated measurements: quantification and implications for sample size. Neuroimage 2008; 42(1): 196–206.
27. Vanhamme L, van den Boogaart A, van Huffel S. Improved method for accurate and efficient quantification of MRS data with use of prior knowledge. J. Magn. Reson. 1997; 129(1): 35–43.
28. Oz G, Alger JR, Barker PB, Bartha R, Bizzi A, Boesch C, Bolan PJ, Brindle KM, Cudalbu C, Dincer A, Dydak U, Emir UE, Frahm J, Gonzalez RG, Gruber S, Gruetter R, Gupta RK, Heerschap A, Henning A, Hetherington HP, Howe FA, Huppi PS, Hurd RE, Kantarci K, Klomp DW, Kreis R, Kruiskamp MJ, Leach MO, Lin AP, Luijten PR, Marjanska M, Maudsley AA, Meyerhoff DJ, Mountford CE, Nelson SJ, Pamir MN, Pan JW, Peet AC, Poptani H, Posse S, Pouwels PJ, Ratai EM, Ross BD, Scheenen TW, Schuster C, Smith IC, Soher BJ, Tkac I, Vigneron DB, Kauppinen RA. Clinical proton MR spectroscopy in central nervous system disorders. Radiology 2014; 270(3): 658–679.
29. Star-Lack J, Spielman D, Adalsteinsson E, Kurhanewicz J, Terris DJ, Vigneron DB. In vivo lactate editing with simultaneous detection of choline, creatine, NAA, and lipid singlets at 1.5 T using PRESS excitation with applications to the study of brain and head and neck tumors. J. Magn. Reson. 1998; 133(2): 243–254.
30. de Graaf R. *In vivo NMR Spectroscopy; Principles and Techniques*, 2nd edn. John Wiley & Sons: Chichester, 2008.
31. de Graaf AA, Luyten PR, den Hollander JA, Heindel W, Bovee WM. Lactate imaging of the human brain at 1.5 T using a double-quantum filter. Magn. Reson. Med. 1993; 30(2): 231–235.
32. Trabesinger AH, Meier D, Boesiger P. In vivo ^{1}H NMR spectroscopy of individual human brain metabolites at moderate field strengths. Magn. Reson. Imaging 2003; 21(10): 1295–1302.
33. Mellon EA, Lee SC, Pickup S, Kim S, Goldstein SC, Floyd TF, Poptani H, Delikatny EJ, Reddy R, Glickson JD. Detection of lactate with a hadamard slice selected, selective multiple quantum coherence, chemical shift imaging sequence (HDMD-SelMQC-CSI) on a clinical MRI scanner: application to tumors and muscle ischemia. Magn. Reson. Med. 2009; 62(6): 1404–1413.
34. Near J, Andersson J, Maron E, Mekle R, Gruetter R, Cowen P, Jezzard P. Unedited in vivo detection and quantification of gamma-aminobutyric acid in the occipital cortex using short-TE MRS at 3 T. NMR Biomed. 2013; 26(11): 1353–1362.
35. Magnitsky S, Belka GK, Sterner C, Pickup S, Chodosh LA, Glickson JD. Lactate detection in inducible and orthotopic Her2/neu mammary gland tumours in mouse models. NMR Biomed. 2013; 26(1): 35–42.
36. He Q, Shungu DC, van Zijl PC, Bhujwalla ZM, Glickson JD. Single-scan in vivo lactate editing with complete lipid and water suppression by selective multiple-quantum-coherence transfer (Sel-MQC) with application to tumors. J. Magn. Reson. Ser. B 1995; 106(3): 203–211.
37. Schaller B, Mekle R, Xin L, Kunz N, Gruetter R. Net increase of lactate and glutamate concentration in activated human visual cortex detected with magnetic resonance spectroscopy at 7 tesla. J. Neurosci. Res. 2013; 91(8): 1076–1083.
38. Mangia S, Tkac I, Logothetis NK, Gruetter R, Van de Moortele PF, Ugurbil K. Dynamics of lactate concentration and blood oxygen level-dependent effect in the human visual cortex during repeated identical stimuli. J. Neurosci. Res. 2007; 85(15): 3340–3346.
39. Lin Y, Stephenson MC, Xin L, Napolitano A, Morris PG. Investigating the metabolic changes due to visual stimulation using functional proton magnetic resonance spectroscopy at 7 T. J. Cerebral Blood Flow Metab. 2012; 32(8): 1484–1495.
40. Harris AD, Roberton VH, Huckle DL, Saxena N, Evans CJ, Murphy K, Hall JE, Bailey DM, Mitsis G, Edden RA, Wise RG. Temporal dynamics of lactate concentration in the human brain during acute inspiratory hypoxia. J. Magn. Reson. Imaging 2013; 37(3): 739–745.
41. Zhu XH, Chen W. Observed BOLD effects on cerebral metabolite resonances in human visual cortex during visual stimulation: a functional (1)H MRS study at 4 T. Magn. Reson. Med. 2001; 46(5): 841–847.
42. McLean MA, Sun A, Bradstreet TE, Schaeffer AK, Liu H, Iannone R, Herman G, Railkar RA, Joubert I, Gillard JH, Price SJ, Griffiths JR. Repeatability of edited lactate and other metabolites in astrocytoma at 3 T. J. Magn. Reson. Imaging 2012; 36(2): 468–475.
43. Wijtenburg SA, Rowland LM, Edden RA, Barker PB. Reproducibility of brain spectroscopy at 7 T using conventional localization and spectral editing techniques. J. Magn. Reson. Imaging 2013; 38(2): 460–467.
44. van de Bank BL, Emir UE, Boer VO, van Asten JJA, Wijnen JP, Kan HE, Öz G, Klomp DJ, Scheenen TW. Multi-center reproducibility of short echo time single voxel ^{1}H MRS of the human brain at 7 T with adiabatic slice-selective refocusing pulses. NMR Biomed. 2015; 28(3): 306–316.